

On the Tail Transition of First Arrival Position Channels: From Cauchy to Exponential Decay

Yen-Chi Lee, *Member, IEEE*

Abstract—While the zero-drift first arrival position (FAP) channel is known to exhibit a Cauchy noise distribution, practical molecular communication systems typically operate under nonzero drift. This letter analyzes the resulting transition in FAP noise behavior from heavy-tailed algebraic decay to exponential regularization. By asymptotically examining the exact FAP distribution, we identify a characteristic propagation distance (CPD) $r_c = \sigma^2/v$ that separates diffusion-dominated and drift-dominated regimes. Numerical results show that in low-drift environments, Gaussian approximations substantially underestimate the achievable rate, whereas the zero-drift Cauchy model provides a physically grounded performance baseline.

Index Terms—Molecular communication (MC), first arrival position (FAP), heavy-tailed noise, Cauchy distribution, achievable rate, spatial interference, phase transition.

I. INTRODUCTION

MOLECULAR communication via diffusion (MCvD) relies on the stochastic motion of information particles to convey messages [1], [2]. While most existing studies focus on first arrival time (FAT), the spatial dimension—namely, the first arrival position (FAP)—offers an alternative information carrier with fundamentally different noise characteristics. In FAT-based systems, information is inherently coupled to random arrival times, and the long temporal tail of diffusion gives rise to severe inter-symbol interference (ISI). In contrast, FAP encodes information in the spatial impact location, rendering arrival time irrelevant and thereby mitigating temporal ISI [3], [4].

Beyond single-link communication, FAP also arises as a fundamental spatial impulse response in molecular MIMO [5] and index modulation [6] systems. Recent surveys on practical molecular communication platforms, including microfluidic testbeds [7], highlight the importance of spatial effects in system implementation and evaluation. In such settings, the statistical behavior of the FAP directly governs *spatial interference* (cross-talk) between adjacent sensing elements, thereby influencing feasible receiver density under interference constraints.

A precise characterization of FAP noise statistics is therefore essential for robust system design. In our previous work [8], we showed that in the zero-drift limit, the FAP channel converges to a multidimensional additive Cauchy noise channel. This result provides a concrete physical realization of stable noise models previously studied in information

This work was supported by the National Science and Technology Council of Taiwan (NSTC 113-2115-M-008-013-MY3). (Corresponding author: Yen-Chi Lee.)

Y.-C. Lee is with the Department of Mathematics, National Central University, Taoyuan, Taiwan (e-mail: yclee@math.ncu.edu.tw).

theory [9], [10], and suggests that variance-based metrics alone may be insufficient for characterizing system performance in such regimes.

The zero-drift Cauchy law, however, represents a singular physical limit in which diffusive transport dominates particle motion [11]. In realistic microfluidic and biological environments, a nonzero drift velocity \mathbf{v} introduces advective transport that progressively regularizes the heavy tail. As a result, the FAP noise undergoes a crossover from algebraic decay to exponential regularization, restoring finite moments. Failing to account for this transition can lead to misleading design conclusions: Gaussian models can underestimate outlier interference at low drift, whereas pure Cauchy models may become overly conservative as drift effects increase.

In this letter, we analyze the drift-induced tail transition of the FAP channel. By asymptotically examining the exact FAP distribution, we identify a *characteristic propagation distance (CPD)* r_c , determined by the diffusion parameter σ^2 and the drift magnitude $v = \|\mathbf{v}\|$. This scale separates diffusion-dominated and drift-dominated regimes, capturing the crossover from Cauchy-like heavy-tailed behavior to exponentially regularized noise. Numerical achievable-rate results further show that in low-drift environments, Gaussian approximations become unreliable, while the zero-drift Cauchy law provides a robust physical baseline for performance evaluation.

The remainder of this letter is organized as follows. Section II introduces the system model and reviews the exact FAP noise distribution under nonzero drift. Section III presents an asymptotic analysis of the tail behavior and identifies the characteristic propagation distance separating diffusion-dominated and drift-dominated regimes. Section IV investigates the implications of this transition for achievable rate and spatial interference. Finally, Section V concludes the letter.

II. SYSTEM MODEL AND EXACT DISTRIBUTION

We consider an MCvD system defined in \mathbb{R}^d Euclidean space. For illustration, the two-dimensional case ($d = 2$) is depicted in Fig. 1. The transmitter (Tx) releases a particle at $\mathbf{X} \in \mathbb{R}^{d-1}$ on a transmitting hyperplane. The particle undergoes Brownian motion with diffusion coefficient D (with variance $\sigma^2 = 2D$) and is subject to a constant drift velocity \mathbf{v} perpendicular to the receiving plane, which is located at a distance $\lambda > 0$ from the transmitter. Let $v = \|\mathbf{v}\|$ denote the drift speed.

Particle arrivals at the receiver (Rx) are characterized by their transverse (lateral) coordinates. Accordingly, the received position on the transverse plane is modeled as $\mathbf{Y} = \mathbf{X} + \mathbf{N}$, where $\mathbf{N} \in \mathbb{R}^{d-1}$ represents the random lateral displacement

TABLE I
SUMMARY OF MAIN NOTATIONS

| Notation | Description |
|--------------|--|
| \mathbf{X} | Transmitted particle position on the transmitting hyperplane, $\mathbf{X} \in \mathbb{R}^{d-1}$. |
| \mathbf{Y} | Received particle position on the transverse (receiving) plane, $\mathbf{Y} \in \mathbb{R}^{d-1}$. |
| \mathbf{N} | Random lateral displacement (additive noise) vector of the FAP channel, defined as $\mathbf{N} = \mathbf{Y} - \mathbf{X}$. |
| \mathbf{n} | Realization of the noise vector \mathbf{N} . |
| X | Scalar transmitted position for the special case $d = 2$. |
| Y | Scalar received position for the special case $d = 2$. |
| N | Scalar noise random variable for $d = 2$, defined as $N = Y - X$. |
| n | Realization of the scalar noise random variable N . |
| D | Diffusion coefficient of the particle motion. |
| σ^2 | Diffusion variance parameter, defined as $\sigma^2 = 2D$. |
| \mathbf{v} | Constant drift velocity vector, perpendicular to the receiving plane. |
| v | Drift speed, defined as $v = \ \mathbf{v}\ $. |
| λ | Separation distance between the transmitting and receiving planes. |
| $\ \cdot\ $ | Euclidean (ℓ_2) norm. |
| r_c | The characteristic propagation distance (CPD) separating diffusion-dominated and drift-dominated regimes, defined as $r_c := \sigma^2/v$. |
| a | Peak-amplitude constraint on the channel input (uniform input $X \sim \mathcal{U}[-a, a]$). |

induced by diffusion. Notice that we use \mathbf{n} to represent the realization of the random vector \mathbf{N} . The *impact position* refers to the transverse location at which a particle first reaches the receiving plane, measured relative to the point directly facing the release position. Thus, the transverse origin ($\mathbf{N} = \mathbf{0}$) corresponds to impacts near the geometric center of the receiver, while large $\|\mathbf{N}\|$ characterize arrivals far from this central region. For the special case $d = 2$, we write $Y = X + N$, since vectors in \mathbb{R}^1 can be identified with scalars.

For clarity, the main notations used throughout this letter are summarized in Table I.

A. The Zero-drift Baseline: Cauchy Distribution

The noise distribution is governed by the drift velocity \mathbf{v} . In the zero-drift limit ($v \rightarrow 0$), the first-arrival position (FAP) noise reduces to a multivariate Cauchy distribution [8]. For the $d = 2$ case (i.e., a scalar noise N on a 1D transverse line), this baseline is given by

$$\lim_{v \rightarrow 0^+} f_N(n | v) = \frac{\lambda}{\pi(n^2 + \lambda^2)}. \quad (1)$$

Equation (1) serves as a physical reference point: in the absence of external flow, the channel exhibits an intrinsically heavy-tailed (algebraic) noise law.

B. The General Case (Non-Zero Drift)

For $v > 0$ (assisting the transmission, as shown in Fig. 1), the exact PDF of the FAP noise for the $d = 2$ case is available in [3] and can be written as

$$f_N(n | v) = \frac{v\lambda}{\pi\sigma^2\sqrt{n^2 + \lambda^2}} \exp\left(\frac{v\lambda}{\sigma^2}\right) K_1\left(\frac{v}{\sigma^2}\sqrt{n^2 + \lambda^2}\right). \quad (2)$$

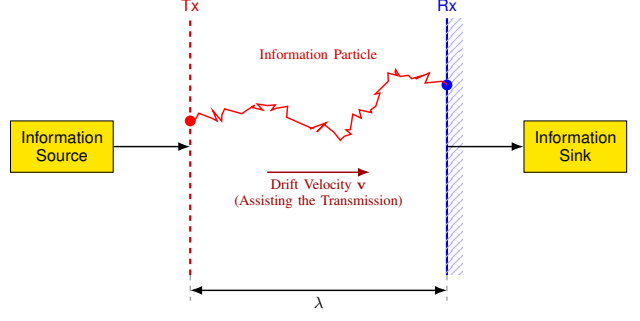


Fig. 1. Abstract FAP channel model featuring hyperplane-shaped transmitter (Tx) and receiver (Rx) pair. The information particle undergoes Brownian motion with diffusion coefficient D and drift velocity \mathbf{v} over a transmission distance λ . The Rx observes the arrival point on the transverse plane.

In (2), $K_1(\cdot)$ denotes the modified Bessel function of the second kind. Although (2) is exact, its special-function form obscures the physical intuition behind tail regularization under drift. We therefore develop an asymptotic analysis in the next section to expose the underlying structure.

III. THE ANATOMY OF THE TAIL: ASYMPTOTIC ANALYSIS

The tail behavior of the noise distribution is governed by the argument of the modified Bessel function appearing in (2). For brevity, we carry out the asymptotic analysis in the two-dimensional case. For later reference, we introduce the radial propagation distance

$$r = r(n) := \sqrt{n^2 + \lambda^2}, \quad (3)$$

and the associated dimensionless parameter

$$z = z(n) := \frac{v}{\sigma^2} r(n) = \frac{r(n)}{r_c}, \quad (4)$$

where $r_c = \sigma^2/v$ is the CPD over which drift and diffusion contribute comparably.

A. Regime 1: The Cauchy Core (Diffusion-Dominated)

We first consider the small- z regime, defined by $z(n) \ll 1$, which corresponds to weak drift or small radial distance $r(n)$. In this regime, the modified Bessel function admits the small-argument asymptotic expansion $K_1(z) \sim 1/z$ (see Appendix A-A). Substituting this approximation into the exact expression (2) gives

$$f_N(n | v) \sim \frac{v\lambda}{\pi\sigma^2 r(n)} \left(\frac{\sigma^2}{v r(n)} \right), \quad z(n) \rightarrow 0 \quad (5)$$

$$\sim \frac{\lambda}{\pi(n^2 + \lambda^2)}, \quad z(n) \rightarrow 0,$$

where we also used $\exp(v\lambda/\sigma^2) \rightarrow 1$ as $v \rightarrow 0$. Therefore, in the small- z limit, the noise distribution reduces to a Cauchy-type law [8], characterized by an algebraic heavy tail of order $O(n^{-2})$. Physically, this regime represents a diffusion-dominated core, in which random thermal motion overwhelms the effect of drift and the channel behavior is well approximated by the zero-drift baseline described in Section II-A.

Taken together, the small- z and large- z regimes reveal the full anatomy of the noise distribution: diffusion gives rise to a

Cauchy-like core near the origin, while drift progressively regularizes the tail by exponentially suppressing large transverse displacements.

B. Regime 2: The Drift-Regularized Tail (Drift-Dominated)

We next consider the large- z regime, defined by $z(n) \gg 1$, which corresponds to large radial distances $r(n)$ or sufficiently strong drift. In this regime, the modified Bessel function admits the large-argument asymptotic expansion

$$K_1(z) \sim \sqrt{\frac{\pi}{2z}} e^{-z}, \quad z \rightarrow \infty \quad (6)$$

(see Appendix A-B). Substituting (6) into the exact expression (2) yields

$$\begin{aligned} f_N(n \mid v) &\sim \frac{v\lambda}{\pi\sigma^2 r(n)} \exp\left(\frac{v\lambda}{\sigma^2}\right) \sqrt{\frac{\pi}{2z(n)}} e^{-z(n)} \\ &= \frac{v\lambda}{\pi\sigma^2 r(n)} \sqrt{\frac{\pi}{2z(n)}} \exp\left(\frac{v}{\sigma^2}(\lambda - r(n))\right), \end{aligned} \quad (7)$$

where we have used $z(n) = (v/\sigma^2)r(n)$. Noting that $\sqrt{1/z(n)} = \sqrt{\sigma^2/(vr(n))}$, the prefactor simplifies accordingly, leading to

$$\begin{aligned} f_N(n \mid v) &\sim \frac{\lambda}{\sigma} \sqrt{\frac{v}{2\pi}} r(n)^{-3/2} \\ &\quad \times \exp\left(\frac{v}{\sigma^2}(\lambda - r(n))\right), \quad z(n) \rightarrow \infty. \end{aligned} \quad (8)$$

Equivalently, in terms of n , this asymptotic form can be written as

$$\begin{aligned} f_N(n \mid v) &\sim \frac{\lambda}{\sigma} \sqrt{\frac{v}{2\pi}} (n^2 + \lambda^2)^{-3/4} \\ &\quad \times \exp\left(\frac{v}{\sigma^2}(\lambda - \sqrt{n^2 + \lambda^2})\right), \quad z(n) \rightarrow \infty. \end{aligned} \quad (9)$$

Moreover, when $|n| \gg \lambda$, we have $r(n) = \sqrt{n^2 + \lambda^2} = |n|\sqrt{1 + (\lambda/n)^2} \sim |n|$. Substituting this into (8) shows that the tail is exponentially regularized as

$$f_N(n \mid v) = \mathcal{O}\left(|n|^{-3/2} \exp\left(-\frac{v}{\sigma^2}|n|\right)\right), \quad |n| \rightarrow \infty. \quad (10)$$

Consequently, $\mathbb{E}|N|^p < \infty$ for all $p > 0$ whenever $v > 0$.

C. The Critical Length Scale

The crossover between the diffusion-dominated Cauchy core and the drift-regularized tail is governed by the dimensionless parameter $z(n) = r(n)/r_c$. In particular, the transition occurs when $z(n)$ is of order unity, i.e.,

$$z(n) \sim \mathcal{O}(1) \Leftrightarrow r(n) \sim r_c. \quad (11)$$

Physically, r_c acts as a cutoff length separating two noise regimes: when $r(n) \ll r_c$ (equivalently, $z(n) \ll 1$), the channel is well approximated by the Cauchy-like diffusion core; when $r(n) \gg r_c$ (equivalently, $z(n) \gg 1$), the tail is exponentially regularized by drift. For large transverse displacements $|n| \gg \lambda$, since $r(n) \sim |n|$, this cutoff can be interpreted directly in terms of the lateral coordinate.

D. Extension to 3D Systems (2D Receiving Plane)

Although the above derivations focus on a two-dimensional system with a one-dimensional receiving line for clarity, the tail anatomy is not dimension-specific. The same mechanism extends naturally to three-dimensional systems with a two-dimensional receiving plane, which are of practical relevance to planar MIMO receiver architectures [5], [6].

In a 3D setting, the noise becomes a vector $\mathbf{N} \in \mathbb{R}^2$, and the exact FAP density depends on the Euclidean propagation distance $r(\mathbf{n}) := \sqrt{\|\mathbf{n}\|^2 + \lambda^2}$ with tail behavior governed by an exponential damping factor of the form $\exp(-vr(\mathbf{n})/\sigma^2)$ [3]. Applying the same asymptotic framework yields two analogous regimes:

- **Core** ($r(\mathbf{n}) \ll r_c$): The distribution converges to a bivariate Cauchy law, exhibiting an algebraic decay $\propto \|\mathbf{n}\|^{-3}$ and providing two spatial degrees of freedom [8].
- **Tail** ($r(\mathbf{n}) \gg r_c$): The distribution undergoes exponential regularization, ensuring the existence of finite moments [3].

Importantly, the same characteristic distance $r_c = \sigma^2/v$ governs the crossover between heavy-tailed and light-tailed behavior, independent of the dimensionality of the receiving geometry.

IV. NUMERICAL IMPLICATIONS OF THE TAIL TRANSITION

The goal of this section is to translate the asymptotic tail-transition analysis developed in Section III into concrete performance implications for MCvD systems. We focus on two key metrics of direct engineering relevance: the *achievable information rate* under a peak-amplitude constraint, and the *spatial interference probability*, which governs cross-talk in planar receiver arrays commonly encountered in molecular MIMO settings.

A. Numerical Setup

Numerical evaluations are performed with transmission distance $\lambda = 10$, peak-amplitude constraint $a = 200$, and diffusion coefficient $D = 100$ (normalized units). The achievable information rate is computed as the mutual information $I(X; Y)$ assuming a uniform input distribution $X \sim \mathcal{U}[-a, a]$, which represents a standard and tractable achievable-rate benchmark under peak constraints.

For comparison, we also include a Gaussian approximation based on a variance-matched additive white Gaussian noise (AWGN) model. Specifically, the corresponding achievable rate is given by

$$R_{\text{Gauss}} = \frac{1}{2} \ln\left(1 + \frac{P_X}{\sigma_N^2(v)}\right), \quad (12)$$

where $\sigma_N^2(v)$ denotes the noise variance computed numerically from the exact distribution in (2), and $P_X = a^2/3$ is the average power of the uniform input. This construction ensures that the Gaussian model is informed of the true second-order noise statistics, thereby isolating the effect of heavy-tailed behavior beyond variance alone.

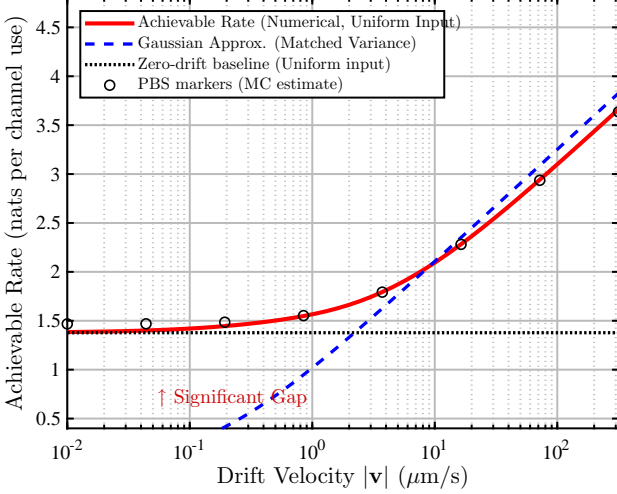


Fig. 2. Achievable information rate of the FAP channel versus drift velocity $|v|$, evaluated under a uniform input constraint. The solid curve shows the numerically evaluated achievable rate, the dashed curve shows the matched-variance Gaussian approximation, and the dotted line indicates the zero-drift baseline obtained under the same uniform-input setting. Discrete markers correspond to PBS simulation results and are included for validation. In the low-drift regime, PBS points may slightly overestimate the achievable rate, which is expected due to the slow convergence of entropy estimators for heavy-tailed noise distributions.

For clarity, we focus on the one-dimensional transverse setting ($d = 2$), which most transparently exhibits the tail-transition phenomenon.

Numerical stabilization: Since the n -dependence of (2) is entirely captured by the Bessel-kernel term, we evaluate a kernel proportional to $K_1(z(n))/r(n)$, which is numerically normalized so that the resulting density integrates to one. For very small drift velocities, the integration grid is refined near $n = 0$ to accurately capture the singular behavior $K_1(z) \sim 1/z$. Throughout, integral-based evaluations are treated as the numerical reference, while particle-based simulations (PBS) are used solely for independent validation and illustration purposes.

B. Achievable Rate Results

Fig. 2 illustrates the achievable information rate as a function of the drift velocity. Three curves are shown: the numerically evaluated achievable rate under a uniform input (solid), the variance-matched Gaussian approximation (dashed), and the zero-drift baseline (dotted), all evaluated under the same input constraint.

Two key observations emerge. First, in the low-drift regime, the achievable rate does not vanish as $v \rightarrow 0$; instead, it stabilizes and approaches a finite baseline value. This behavior indicates that reliable information transmission remains possible in diffusion-dominated regimes, even in the absence of drift assistance.

Second, the Gaussian approximation significantly underestimates the achievable rate at low drift. As the FAP noise distribution approaches the Cauchy limit, its variance diverges, causing variance-based Gaussian models to predict vanishing rates, despite the presence of substantial information-carrying

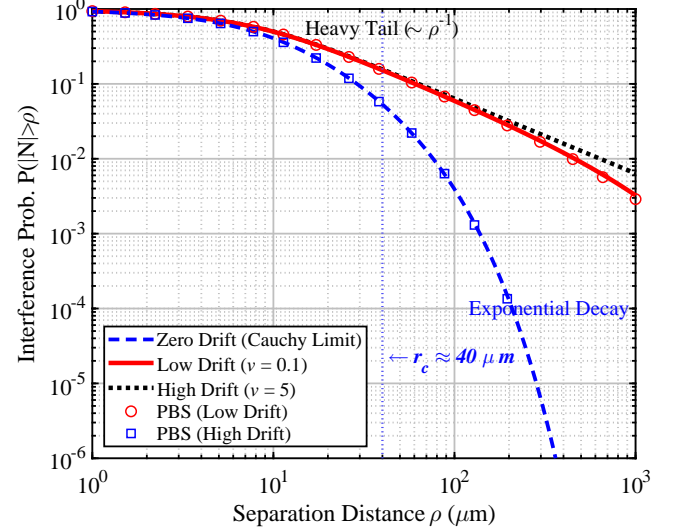


Fig. 3. Spatial interference probability $P(|N| > \rho)$ versus lateral separation distance ρ . Theoretical curves are obtained from the exact FAP distribution, while discrete markers indicate PBS results based on exact first-passage-time sampling. The characteristic distance r_c delineates the crossover from diffusion-dominated algebraic decay to drift-regularized exponential decay.

capability. This discrepancy highlights the fundamental inadequacy of Gaussian approximations for heavy-tailed FAP channels.

Taken together, these results show that in diffusion-dominated regimes, characterized by r_c exceeding the relevant array spacing or aperture scale, variance-based Gaussian models can be overly pessimistic and fail to capture the true operational limits of the channel.

Discrete PBS results included in Fig. 2 serve as an independent validation of the numerical evaluation. In the low-drift regime, minor deviations from the benchmark curve are expected due to the slow convergence of finite-sample entropy estimators under heavy-tailed noise. As the drift increases and the FAP tail becomes exponentially regularized, PBS estimates rapidly converge to the theoretical predictions.

C. Impact on Spatial Interference

To quantify spatial cross-talk in molecular MIMO systems, we consider the spatial interference probability

$$P_{\text{int}}(\rho) = \mathbb{P}(|N| > \rho), \quad (13)$$

which represents the likelihood that a particle arrives beyond a lateral separation distance ρ from its intended receiver location.

Fig. 3 presents numerical results for both zero-drift and nonzero-drift scenarios. In the zero-drift case, the transverse FAP noise N follows the Cauchy distribution given in (1). The corresponding interference probability therefore follows directly from integration of the Cauchy density,

$$\begin{aligned} P_{\text{int}}(\rho) &= \mathbb{P}(|N| > \rho) = 2 \int_{\rho}^{\infty} f_N(n) dn \\ &= \frac{2}{\pi} \left[\arctan\left(\frac{n}{\lambda}\right) \right]_{\rho}^{\infty} = 1 - \frac{2}{\pi} \arctan\left(\frac{\rho}{\lambda}\right). \end{aligned} \quad (14)$$

For large separation distances $\rho \gg \lambda$, this expression admits the asymptotic form

$$P_{\text{int}}(\rho) \sim \frac{2\lambda}{\pi\rho}, \quad (15)$$

confirming the algebraic ρ^{-1} decay characteristic of diffusion-dominated transport.

For nonzero drift, the interference probability is evaluated numerically as

$$P_{\text{int}}(\rho) = 2 \int_{\rho}^{\infty} f_N(n \mid v) dn, \quad (16)$$

where symmetry of the FAP distribution is used to simplify the evaluation. The resulting curves exhibit a systematic change in spatial interference behavior as the drift strength increases. When the drift is sufficiently strong, the interference probability decreases rapidly once the separation distance exceeds the characteristic scale $r_c = \sigma^2/v$. In this regime, r_c provides a natural guideline for choosing receiver spacing to effectively suppress cross-talk in dense arrays. In contrast, when the drift is weak and r_c exceeds the relevant system dimensions, the interference probability remains close to the zero-drift Cauchy baseline, reflecting persistent long-range cross-talk in diffusion-dominated settings.

V. CONCLUSION

This letter analyzed the drift-induced transition of FAP noise from a heavy-tailed Cauchy law to an exponentially regularized distribution. By asymptotically examining the exact FAP density, we identified the characteristic propagation distance $r_c = \sigma^2/v$ as the boundary separating diffusion-dominated and drift-dominated regimes.

Numerical results showed that in low-drift environments, FAP-based communication remains robust despite variance divergence, with achievable rates well captured by the zero-drift uniform-input baseline, while Gaussian approximations become unreliable. The cutoff scale r_c further provides a simple and physically interpretable guideline for assessing feasible receiver spacing in planar molecular MIMO systems under spatial interference constraints. Overall, this framework offers a unified physical interpretation of tail regularization in FAP channels and establishes a principled baseline for spatial modulation design in drift-assisted molecular communications.

APPENDIX A

ASYMPTOTIC BEHAVIOR OF THE MODIFIED BESSEL FUNCTION

This appendix summarizes the asymptotic behavior of the modified Bessel function of the second kind, which underlies both the diffusion-dominated core and the drift-regularized tail behaviors analyzed in the main text.

A. Small-Argument Regime ($z \rightarrow 0^+$)

For the modified Bessel function $K_\nu(z)$ with order $\nu > 0$, its small-argument asymptotic expansion is given by [12, Eq. (9.6.9)]

$$K_\nu(z) \sim \frac{1}{2} \Gamma(\nu) \left(\frac{2}{z} \right)^\nu, \quad z \rightarrow 0^+, \quad (17)$$

up to lower-order correction terms.

In particular, for $\nu = 1$, since $\Gamma(1) = 1$, the leading-order behavior reduces to

$$K_1(z) \sim \frac{1}{z}, \quad z \rightarrow 0. \quad (18)$$

This algebraic $O(z^{-1})$ scaling gives rise to the Cauchy-type diffusion-dominated core of the FAP noise distribution discussed in Section III.

B. Large-Argument Regime ($z \rightarrow \infty$)

For fixed order ν , the large-argument asymptotic expansion of $K_\nu(z)$ is given by [12, Eq. (9.7.2)]

$$K_\nu(z) \sim \sqrt{\frac{\pi}{2z}} e^{-z} \left(1 + \mathcal{O}\left(\frac{1}{z}\right) \right), \quad z \rightarrow \infty. \quad (19)$$

In particular, for $\nu = 1$, the leading-order behavior reduces to

$$K_1(z) \sim \sqrt{\frac{\pi}{2z}} e^{-z}, \quad z \rightarrow \infty. \quad (20)$$

This exponential decay governs the drift-regularized tail of the FAP noise distribution and leads to the suppression of large transverse displacements described in Section III.

REFERENCES

- [1] I. F. Akyildiz, F. Brunetti, and C. Blázquez, "Nanonetworks: A new communication paradigm," *Comput. Netw.*, vol. 52, no. 12, pp. 2260–2279, Aug. 2008.
- [2] N. Farsad, H. B. Yilmaz, A. Eckford, C.-B. Chae, and W. Guo, "A comprehensive survey of recent advancements in molecular communication," *IEEE Communications Surveys & Tutorials*, vol. 18, no. 3, pp. 1887–1919, 2016.
- [3] Y.-C. Lee, Y.-F. Lo, J.-M. Wu, and M.-H. Hsieh, "Characterizing First Arrival Position channels: Noise distribution and capacity analysis," *IEEE Trans. Commun.*, vol. 72, no. 7, pp. 4010–4025, Jul. 2024.
- [4] N. Pandey, R. K. Mallik, and B. Lall, "Molecular communication: The First Arrival Position channel," *IEEE Wireless Commun. Lett.*, vol. 8, no. 2, pp. 508–511, Apr. 2018.
- [5] B.-H. Koo, C. Lee, H. B. Yilmaz, N. Farsad, A. Eckford, and C.-B. Chae, "Molecular MIMO: From theory to prototype," *IEEE J. Sel. Areas Commun.*, vol. 34, no. 3, pp. 600–614, Mar. 2016.
- [6] M. C. Gursoy, E. Basar, A. E. Pusane, and T. Tugcu, "Index modulation for molecular communication via diffusion systems," *IEEE Trans. Commun.*, vol. 67, no. 5, pp. 3337–3350, May 2019.
- [7] M. Hamidović, S. Angerbauer, D. Bi, Y. Deng, T. Tugcu, and W. Haselmayr, "Microfluidic systems for molecular communications: A review from theory to practice," *IEEE Trans. Mol. Biol. Multi-Scale Commun.*, 2024.
- [8] Y.-C. Lee and M.-H. Hsieh, "On the capacity of zero-drift first arrival position channels in diffusive molecular communication," in *Proc. IEEE Int. Conf. Commun. (ICC)*, Denver, CO, USA, Jun. 2024, pp. 3672–3677.
- [9] J. Fahs and I. Abou-Faycal, "Information measures, inequalities and performance bounds for parameter estimation in impulsive noise environments," *IEEE Transactions on Information Theory*, vol. 64, no. 3, pp. 1825–1844, 2017.
- [10] S. Verdú, "The Cauchy distribution in information theory," *Entropy*, vol. 25, no. 2, p. 346, Feb. 2023.
- [11] R. B. Bird, W. E. Stewart, and E. N. Lightfoot, *Transport Phenomena*, 2nd ed. John Wiley & Sons, 2007.
- [12] M. Abramowitz and I. A. Stegun, *Handbook of Mathematical Functions: with Formulas, Graphs, and Mathematical Tables*. Courier Corporation, 1964, vol. 55, Tenth Printing, December 1972, with corrections.